Quantum-Enhanced Heat Engine Based on Superabsorption

Shunsuke Kamimura,[1,2,*] Hideaki Hakoshima,[1,3] Yuichiro Matsuzaki,[1,†] Kyo Yoshida,[2] and Yasuhiro Tokura[2,4,‡]
[1]Research Center for Emerging Computing Technologies, National Institute of Advanced Industrial Science and Technology (AIST), 1-1-1 Umezono, Tsukuba, Ibaraki 305-8568, Japan
[2]Faculty of Pure and Applied Sciences, University of Tsukuba, Tsukuba 305-8571, Japan
[3]Center for Quantum Information and Quantum Biology, Osaka University, 1-2 Machikaneyama, Toyonaka 560-0043, Japan
[4]Tsukuba Research Center for Energy Materials Science (TREMS), Tsukuba 305-8571, Japan

(Received 29 June 2021; revised 21 December 2021; accepted 21 March 2022; published 3 May 2022)

We propose a quantum-enhanced heat engine with entanglement. The key feature of our scheme is superabsorption, which facilitates enhanced energy absorption by entangled qubits. Whereas a conventional engine with N separable qubits provides power with a scaling of $P = \Theta(N)$, our engine uses superabsorption to provide power with a quantum scaling of $P = \Theta(N^2)$. This quantum heat engine also exhibits a scaling advantage over classical ones composed of N-particle Langevin systems. Our work elucidates the quantum properties allowing for the enhancement of performance.

DOI: 10.1103/PhysRevLett.128.180602

Quantum properties such as entanglement are important to realize desirable performance of devices. Quantifying the performance of quantum devices often requires investigation of how the performance scales with the number of qubits N. For example, a quantum computer can solve certain problems exponentially faster than the best known classical algorithm [1–3], where the size of the problem corresponds to the number of qubits. In quantum sensing, the uncertainty in the target parameter scales as $\Theta(N^{-0.5})$ using separable qubits and $\Theta(N^{-1})$ using entangled qubits [4–6].

Since the Industrial Revolution, the properties and performances of heat engines have been successfully described using a long-standing framework called thermodynamics [7,8]. In previous decades, thermodynamics has been generalized to classical small systems far from equilibria [9], and these systems cannot be understood without the information point of view [10–12]. This framework is referred to as stochastic thermodynamics. It provides tighter constraints on the properties of systems than conventional thermodynamics, such as fluctuation theorems [13–16] and trade-off relations [17,18], and it is applicable to various research topics such as chemical reactions [19,20] and biological systems [21,22].

The development of microfabrication techniques has allowed devices to acquire quantum characteristics, thereby facilitating various information processes that are much more efficient than conventional strategies, as mentioned above. Thus, there is a rapidly growing demand to establish thermodynamics generalized to quantum systems [23,24]. In this framework, which is called quantum thermodynamics [25], open quantum systems are considered as working media [26,27], and relevant quantities such as work and heat are defined by analogy with classical systems [28]. Although the generalization of thermodynamics to quantum systems seems straightforward, it significantly extends the scope of thermodynamics not only to heat engines composed of nanodevices [29–33] but also to biological systems such as photosynthesis systems [34], as quantum systems can provide a richer set of possibilities. In particular, the quantum version of the trade-off relation between power and efficiency is described by a measure of quantum coherence, which has no counterpart in classical physics [35].

In the quantum thermodynamics, one of the main issues is defining scaling advantages of quantum heat engines over classical ones [35–39]. In Ref. [35], Tajima and Funo use an abstract system that has only two energies, and there are N_d degenerate states at each energy. They show that quantum coherence among degenerate states can enhance the scaling of a power with the number of degeneracy while the value of an efficiency is fixed. This demonstrates the scaling enhancement of quantum engines at a finite temperature where the degeneracy of the system seems to play a role in defining the enhancement.

However, the model of Ref. [35] is so abstract that we cannot easily understand the physics and mechanism behind the quantum enhancement. Moreover, due to such nature of their model, it is not straightforward to find a physical counterpart of their model. For a better interpretation of the quantum phenomena, it is preferable to seek another concrete model that provides the quantum enhancement with a physically realizable setting.

Here, we propose a quantum heat engine with a qubit-based model that is relevant and applicable to many quantum information protocols. The key feature of our model is a collective quantum phenomenon called superabsorption, which allows for efficient energy exchange

between the qubits and environment [40–43]. By using a physically realizable system, we show how the enhanced power scaling of $\Theta(N^2)$ and the fixed value of the efficiency can be achieved with N entangled qubits at the same time, whereas a conventional engine with N separable qubits provides a power with a scaling of $\Theta(N)$. Our engine also beats classical engines composed of N particles obeying a Langevin equation where the power scales as $\Theta(N)$ [17,44]. Considering the microscopic model of the heat engine, we add the understanding of quantum-enhanced performance. More specifically, our results reveal that the description of the enhancement by the degeneracy is not generic; rather the origin of the enhancement can be understood by a *connectivity* between quantum states where the system dynamics takes place.

Superabsorption.—Superabsorption [40–43] is the reverse process of superradiance. In superradiance, a collective emission is observed in an N-qubit system near the middle of the Dicke ladder [45–48]. However, an energy emission process is more dominant than an energy absorption process when a system is coupled with a white-noise environment; thus, it is not straightforward to observe superabsorption in a natural environment. To overcome this limitation, quantum control techniques can be used to enhance the absorption process. In particular, an interacting qubit system is coupled with a controlled environment for transition rate engineering; then, superabsorption can be achieved where the target two states chosen from the middle of the Dicke ladder have an enhanced transition [40].

We introduce a Hamiltonian for superabsorption. In this system, we assume that the environment can be controlled by reservoir engineering. In particular, we consider a case in which the qubits are coupled with a leaky cavity [49,50], and this coupling induces an energy relaxation on the qubits with a Lorentzian form factor [51,52]. The Hamiltonian $\hat{H}_{\rm tot}$ of the total system is given by

$$\hat{H}_{\rm tot} = \hat{H}_N + \hat{H}_E + \hat{H}_{\rm int}, \tag{1}$$

$$\begin{aligned}
\hat{H}_N &= \omega_A \hat{J}_z + \Omega \hat{J}_z^2, \\
\hat{H}_E &= \int_{-\infty}^{\infty} dk\, \omega_k \hat{B}_k^\dagger \hat{B}_k, \qquad \omega_k = |k|, \\
\hat{H}_{\rm int} &= \int_{-\infty}^{\infty} dk (\hat{J}_+ + \hat{J}_-)\,(\xi(\omega_k)\hat{B}_k + \xi^*(\omega_k)\hat{B}_k^\dagger), \\
\xi(\omega) &= \sqrt{\frac{\Delta\omega}{2\pi}} \frac{g}{\omega - \omega_c - i\Delta\omega/2},
\end{aligned} \tag{2}$$

where $\hat{H}_N$ ($\hat{H}_E$) denotes a Hamiltonian for the N-qubit system (environment) and $\hat{H}_{\rm int}$ denotes an interaction Hamiltonian between the system and environment. In our system, all N qubits have the same frequency ω_A and interact with each other in an all-to-all manner with strength Ω. For the engineered bosonic environment, a mode with wave number k (and energy $\omega_k = |k|$) is collectively coupled to the N-qubit system with the complex function $\xi(\omega_k)$. The cavity, with frequency ω_c, is coupled to the N-qubit system with strength g, and $\Delta\omega$ is the decay rate of the cavity. The bosonic operators $\hat{B}_k$ satisfy the commutation relations $[\hat{B}_k, \hat{B}_{k'}^\dagger] = \delta(k - k')$. The collective operators $\hat{J}_z$ and $\hat{J}_\pm$ are defined by summations of the Pauli operators for all the qubits as $\hat{J}_z = \frac{1}{2}\sum_{i=1}^N \hat{\sigma}_z^{(i)}$ and $\hat{J}_\pm = \sum_{i=1}^N \hat{\sigma}_\pm^{(i)}$, where $\hat{\sigma}_z = |e\rangle\langle e| - |g\rangle\langle g|$, $\hat{\sigma}_+ = |e\rangle\langle g|$, $\hat{\sigma}_- = (\hat{\sigma}_+)^\dagger$, and $|e\rangle$ ($|g\rangle$) denotes the excited (ground) state of a qubit. By introducing another collective operator $\hat{J}^2$ that represents the total angular momentum, we define $|J, M\rangle$ as a Dicke state, which is a simultaneous eigenstate of the operators $\hat{J}^2$ and $\hat{J}_z$ with eigenvalues $J(J+1)$ and M, respectively [45].

When the initial state of the system belongs to a subspace spanned by the Dicke states $|M\rangle = |(N/2), M\rangle$ having the maximum total angular momentum, the dynamics under consideration is totally confined in the same subspace. This subspace is called the Dicke ladder, within which the Hamiltonian $\hat{H}_N$ is diagonal as

$$\hat{H}_N = \sum_M E_M |M\rangle\langle M|, \qquad E_M = \omega_A M + \Omega M^2. \tag{3}$$

In addition, we define an energy difference $\Delta_M = E_M - E_{M-1} = \omega_A + (2M-1)\Omega$ and a transition frequency $\omega_M = |\Delta_M|$ between the Dicke states $|M\rangle$ and $|M-1\rangle$ $(M = -(N/2), -(N/2)+1, \ldots, (N/2))$.

By adopting the standard Born-Markov and rotating-wave approximation, for an N-qubit quantum state $\hat{\rho}_S$ that is diagonal in the Dicke states $\{|M\rangle\}$, we can derive the following Gorini-Kossakowski-Sudarshan-Lindblad (GKSL) master equation [40]:

$$\frac{d\hat{\rho}_S}{dt} = \sum_M a_M (\Gamma_M^\downarrow \mathcal{D}[\hat{L}_M^\downarrow][\hat{\rho}_S] + \Gamma_M^\uparrow \mathcal{D}[\hat{L}_M^\uparrow][\hat{\rho}_S]). \tag{4}$$

For a positive Δ_M, the factor $\Gamma_M^\downarrow = \kappa_M(1+n_M)$ ($\Gamma_M^\uparrow = \kappa_M n_M$) is a transition coefficient for the dynamics $|M\rangle \mapsto |M-1\rangle$ ($|M-1\rangle \mapsto |M\rangle$), where $n_M = 1/(e^{\beta\omega_M} - 1)$ is defined as the Bose-Einstein occupation number with an inverse temperature β and $\kappa_M = 4\pi|\xi(\omega_M)|^2$ is the value of the spectral density at frequency ω_M. The dynamics $|M\rangle \mapsto |M-1\rangle$ ($|M-1\rangle \mapsto |M\rangle$) is induced by a Lindblad operator $\hat{L}_M^\downarrow = |M-1\rangle\langle M|$ ($\hat{L}_M^\uparrow = (\hat{L}_M^\downarrow)^\dagger$). (For a negative Δ_M, the definitions of the coefficients and the Lindblad operators are, respectively, interchanged.) In a two-level system defined as $\mathcal{H}_M = \{|M\rangle, |M-1\rangle\}$, a detailed-balance condition $\Gamma_M^\downarrow/\Gamma_M^\uparrow = e^{\beta\Delta_M}$ is satisfied for each M. The superoperator $\mathcal{D}$ is given by $\mathcal{D}[\hat{L}][\hat{\rho}] = \hat{L}\hat{\rho}\hat{L}^\dagger - \frac{1}{2}(\hat{L}^\dagger\hat{L}\hat{\rho} + \hat{\rho}\hat{L}^\dagger\hat{L})$ for arbitrary

operators $\hat{L}$ and $\hat{\rho}$, and $a_M = [(N/2)+M][(N/2)-M+1]$. In particular, a_M quantifies the enhancement of the transition rate of $\mathcal{H}_M$. Specifically, for an odd number N (as assumed throughout this Letter), the label $M = 1/2$ gives us the largest factor $a_{1/2} = (N+1)^2/4$. Thus, we obtain the maximum enhancement of the transition rate within a subspace $\mathcal{H}_{1/2} = \{|1/2\rangle, |-1/2\rangle\}$, which we call the effective two-level system (E2LS). It is worth noting that $|1/2\rangle$ and $|-1/2\rangle$ are highly entangled states used for many other applications in quantum information processing [45,46,53–59].

The key aspect of superabsorption is to confine the dynamics within the E2LS. Such a confinement can be realized by setting $\Omega \gg \Delta\omega$ and $\omega_c = \omega_{1/2}$ (which we adopt throughout this Letter). In this case, owing to the frequency selectivity, the environment is strongly coupled only with the E2LS, and the energy absorption transition $|-1/2\rangle \mapsto |1/2\rangle$ becomes much more relevant than the energy emission process $|-1/2\rangle \mapsto |-3/2\rangle$.

Heat engine based on superabsorption.—Here, we describe our protocol of the quantum-enhanced heat engine based on superabsorption (see Fig. 1). The N-qubit system is a working medium in our scheme. We employ a high-temperature bath and a low-temperature bath. The inverse temperature and cavity frequency of the high(low)-temperature bath are $\beta_H(\beta_C)$ and $\omega_c^H(\omega_c^C)$, respectively. The initial state $\hat{\rho}_S(0)$ is diagonal in the Dicke states $\{|M\rangle\}_M$ as $\hat{\rho}_S(0) = \sum_M p_M(0)|M\rangle\langle M|$. A cycle of the heat engine consists of four strokes as follows: *Stroke 1: Thermalization with a high-temperature bath.* The N-qubit system is coupled with a high-temperature bath β_H for a period τ_H. During this process, the qubits are resonant with the cavity as $\omega_c^H = \omega_A^H$, and the energy of the Dicke state $|M\rangle$ is given by $E_M^H = M\omega_A^H + M^2\Omega$. The dynamics of this thermalization stroke from $\hat{\rho}_S(0)$ to $\hat{\rho}_S(\tau_H) = \sum_M p_M(\tau_H)|M\rangle\langle M|$ is governed by Eq. (4), and the change in the energy of the N-qubit system is interpreted as a heat input Q_H to the system: $Q_H = \sum_M E_M^H[p_M(\tau_H) - p_M(0)]$. *Stroke 2: Quenching of the qubit frequency* $\omega_A^H \mapsto \omega_A^C$. After decoupling all the qubits from the heat bath β_H, the qubit frequency is simultaneously changed from ω_A^H to ω_A^C. We assume that this is performed in a much shorter time than the time required for a single cycle of our engine. As the instantaneous Hamiltonian $\hat{H}_N$ always commutes with $\hat{\rho}_S(\tau_H)$, the state remains in $\hat{\rho}_S(\tau_H)$. For this stroke, the energy change of the system is interpreted as a work output $W_{\rm out}$ from the system: $W_{\rm out} = \sum_M (E_M^H - E_M^C)p_M(\tau_H)$. Here, $E_M^C = M\omega_A^C + M^2\Omega$ is the energy of $|M\rangle$ after this quenching stroke. *Stroke 3: Thermalization with a low-temperature bath.* The N-qubit system is coupled with a low-temperature bath β_C for a period τ_C, and a resonant condition $\omega_c^C = \omega_A^C$ is assumed. The dynamics in this stroke is described by $\hat{\rho}_S(\tau_H) \mapsto \hat{\rho}_S(\tau) = \sum_M p_M(\tau)|M\rangle\langle M|$ ($\tau = \tau_H + \tau_C$). Similar to Stroke 1, a heat output Q_C to the bath is defined as $Q_C = \sum_M E_M^C[p_M(\tau_H) - p_M(\tau)]$. *Stroke 4: Quenching of the qubit frequency* $\omega_A^C \mapsto \omega_A^H$. After decoupling all the qubits from the heat bath β_C, the qubit frequency is simultaneously changed from ω_A^C to ω_A^H. Again, we assume that we can ignore the quenching time for this stroke. For the same reason as that in the case of Stroke 2, the quantum state remains in $\hat{\rho}_S(\tau)$ during this stroke, and a work input $W_{\rm in}$ to the system is defined as $W_{\rm in} = \sum_M (E_M^H - E_M^C)p_M(\tau)$.

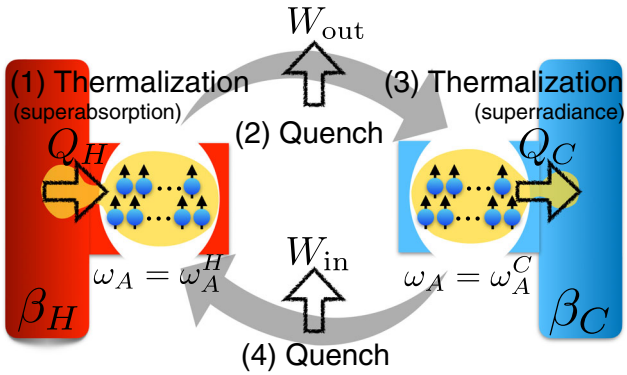

FIG. 1. Schematic of protocol for heat engine based on superabsorption. N qubits interact with a cavity coupled with a thermal bath. This configuration is useful for tailoring the properties of the environment for the qubits. By repeated thermalization of the qubits and quenching of the qubit frequency, we can extract the work. A heat engine with separable states corresponds to a case with $N = 1$, and we can operate N separable engines in parallel.

We define the efficiency η and power output P of the heat engine cycle as

$$\eta = \frac{W_{\rm ext}}{Q_H}, \qquad P = \frac{W_{\rm ext}}{\tau}, \tag{5}$$

where $W_{\rm ext} = W_{\rm out} - W_{\rm in}$ denotes the extractable work. We introduce an efficiency deficit as $\Delta\eta = \eta_C - \eta$, where $\eta_C = 1 - \beta_H/\beta_C$ is the Carnot efficiency.

Now, we explain the choice of parameters. We set the thermalization periods as $\tau_H = \epsilon/(a_{1/2}\Gamma_{1/2}^{H\downarrow})$ and $\tau_C = \epsilon/(a_{1/2}\Gamma_{1/2}^{C\downarrow})$, where ϵ denotes a positive dimensionless constant. Then, the cycle period $\tau = \tau_H + \tau_C$ scales as $\tau = \Theta(N^{-2})$. For the subsequent analytical discussion, ϵ should be much smaller than one so that higher-order terms $O(\epsilon^2)$ can be ignored. Moreover, we choose the initial state $\hat{\rho}_S(0) = \sum_M p_M(0)|M\rangle\langle M|$ as

$$p_{-1/2}(0) = \frac{2}{2 + e^{-\beta_H\omega_A^H} + e^{-\beta_C\omega_A^C}}, \tag{6}$$

where $p_{1/2}(0) = 1 - p_{-1/2}(0)$ and $p_M(0) = 0$ for $M \neq \frac{1}{2}, -\frac{1}{2}$. This choice is for an analytical form of the power and efficiency, as will be described later. Now, we

consider a ratio $\chi_{\rm conf}$ between $p_{1/2}(\tau_H)-p_{1/2}(0)$ and $p_{-3/2}(\tau_H)-p_{-3/2}(0)$, which quantifies the population change in the E2LS compared with that in $|-3/2\rangle$. It is worth noting that, because we consider a low-temperature condition ($\beta_H\omega_A^H,\beta_C\omega_A^C \gg 1$), the population of $|3/2\rangle$ is negligible. According to this analysis, we choose parameters that satisfy the following condition:

$$\chi_{\rm conf}=\left[1+16\left(\frac{\Omega}{\Delta\omega}\right)^2\right]\frac{e^{-\beta_H\omega_A^H}-e^{-\beta_C\omega_A^C}}{2}\gg 1. \quad (7)$$

Thus, as long as this condition (7) is satisfied, the dynamics of the system is nearly confined in the E2LS. The condition (7) implies that both the reservoir engineering and the coupling between qubits are essential, because we cannot satisfy this condition with either a white-noise environment ($\Delta\omega\to\infty$) or noninteracting qubits ($\Omega=0$). Therefore, the concept of superabsorption is crucial for realizing the proposed engine.

Here, we consider a simplified scenario in which the dynamics is perfectly confined in the E2LS to calculate the power and efficiency, although we will discuss more realistic cases with a finite leakage from the E2LS later. When we adopt the initial state described by Eq. (6) and $p_{1/2}(0)=1-p_{-1/2}(0)$, by disregarding both the leakage and the higher-order terms $O(\epsilon^2)$, we can construct a closed trajectory of the quantum state after a heat engine cycle; the populations of $|1/2\rangle$ and $|-1/2\rangle$ do not change after the cycle. Then, we obtain the following forms of the efficiency deficit and power, respectively:

$$\Delta\eta_{\rm E2LS}=\frac{\omega_A^C}{\omega_A^H}-\frac{\beta_H}{\beta_C}\geq 0, \quad (8)$$

$$P_{\rm E2LS}=a_{1/2}P_{N=1}, \quad (9)$$

where the power output $P_{N=1}$ for a one-qubit system is explicitly given by

$$P_{N=1}=\frac{\gamma_P(e^{-\beta_H\omega_A^H}-e^{-\beta_C\omega_A^C})}{4-(e^{-\beta_H\omega_A^H}+e^{-\beta_C\omega_A^C})^2}(\omega_A^H-\omega_A^C). \quad (10)$$

Here, $\gamma_P=8g^2/\Delta\omega$ represents a modified relaxation rate owing to the Purcell effect [51,52,60]. From Eq. (9), because we have $a_{1/2}=\frac{1}{4}(N+1)^2$, we obtain the quantum-enhanced performance $P=\Theta(N^2)$ at a finite temperature, which is significantly different from the performance $P_{\rm sep}=\Theta(N)$ obtained with N separable qubits.

Here, we consider what properties of quantum systems contribute to the scaling advantage of performance. The Dicke state $|1/2\rangle$ ($|-1/2\rangle$) with N qubits is an equal-weight superposition of all computational bases with $(N+1)/2$ ($(N-1)/2$) qubits in $|e\rangle$ and $(N-1)/2$ ($(N+1)/2$) qubits in $|g\rangle$, and the energies corresponding to $|1/2\rangle$ and $|-1/2\rangle$ both have an exponentially large degeneracy given by ${}_NC_{(N+1)/2}\sim 2^N/\sqrt{N}$. However, by applying the jump operator of Eq. (4), which flips only one spin, to a computational basis of $|1/2\rangle$ ($|-1/2\rangle$), we have only $[(N+1)/2]$ bases of $|-1/2\rangle$ ($|1/2\rangle$), and we define this value as a *connectivity*. This value provides us a matrix element of the operator $\hat{J}_+$ between $|1/2\rangle$ and $|-1/2\rangle$, and its square gives the resulting scaling factor of the transition rate $a_{1/2}=\frac{1}{4}(N+1)^2$ in our system. This shows that, for the quantum enhancement, the degeneracy is not generic; rather the connectivity of the quantum states between one degenerated subspace and another induced by the system-environment interaction is crucial. Moreover, our results provide a unified understanding of both our model and that of Tajima and Funo [35]. In their case, the number of connectivity coincides with that of degeneracy, and thus our results lead to a conclusion that their scaling advantage also comes from the number of connectivity [61].

Now, we consider the dependence of the confinement performance $\chi_{\rm conf}$ on the efficiency deficit $\Delta\eta_{\rm E2LS}$ in our engine. In particular, we consider the case in which we tune only ω_A^C to change $\Delta\eta_{\rm E2LS}$. Then, $\chi_{\rm conf}$ can be rewritten as

$$\chi_{\rm conf}=\frac{\beta_C\omega_A^H}{2e^{\beta_H\omega_A^H}}\left[1+16\left(\frac{\Omega}{\Delta\omega}\right)^2\right]\Delta\eta_{\rm E2LS}+O(\Delta\eta_{\rm E2LS}^2). \quad (11)$$

This implies that $\chi_{\rm conf}$ is linearly dependent on $\Delta\eta_{\rm E2LS}$. When we take the Carnot limit $\Delta\eta_{\rm E2LS}\to 0$ by tuning ω_A^C and fixing the other parameters, $\chi_{\rm conf}$ approaches zero, and the system is no longer confined in the E2LS. Meanwhile, for a fixed $\Delta\eta_{\rm E2LS}$, by choosing a larger value of $\Omega/\Delta\omega$, we can maintain the confinement condition of $\chi_{\rm conf}\gg 1$. Thus, controlling the parameter $\Omega/\Delta\omega$ via reservoir engineering is crucial for our scheme.

Next, we investigate a trade-off relation between the power and the efficiency of our engine. Tajima and Funo derived a trade-off relation $P/\Delta\eta\leq\mathcal{B}_{\rm TF}$ for quantum heat engines described by GKSL master equations, where the upper bound $\mathcal{B}_{\rm TF}$ quantifies a (time-averaged) measure of quantum coherence during the heat engine cycle [35]. To the best of our knowledge, our study is the first to apply the general formula to an N-qubit system, and we prove that $\mathcal{B}_{\rm TF}=\Theta(N^2)$. Thus, our heat engine scheme attains this upper bound in terms of the scaling with N. For a classical model of heat bath described by a Langevin equation, there is a known bound of $P/\Delta\eta\leq\mathcal{B}_{\rm SST}=\Theta(N)$ for an N-particle system, as discussed in Refs. [17,44]. Therefore, the trade-off performance $P/\Delta\eta=\Theta(N^2)$ of our heat engine reflects the scaling advantage over such classical engines as well [61].

Numerical results.—Here, we present numerical results on the performance of our heat engine under the effect of a finite leakage from the E2LS. First, we estimate the number of cycles $n_{\rm conf}$ during which the quantum state is

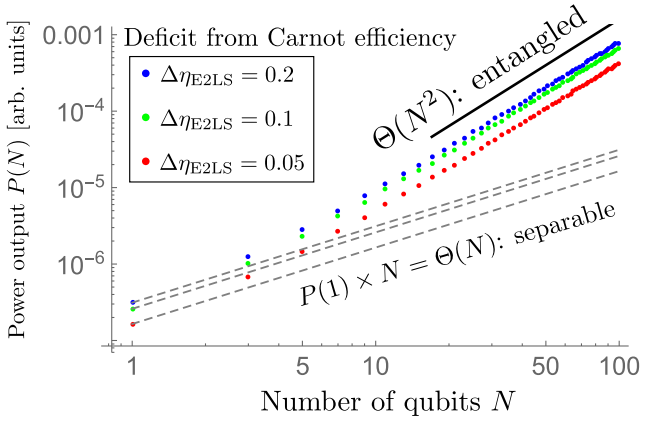

FIG. 2. Dependency of the power output $P(N)$ on the number of qubits N. The numerical values of the parameters are chosen as $\omega_A^H/2\pi = 1$ GHz, $\Omega/2\pi = 31$ MHz, $T_H = (k_B\beta_H)^{-1} = 20$ mK, $T_C = (k_B\beta_C)^{-1} = 10$ mK, $g/2\pi = 10$ kHz, $\Delta\omega/2\pi = 1$ MHz, and $\epsilon = 0.001$. To change the efficiency as $\Delta\eta_{\mathrm{E2LS}} = 0.2$, 0.1, and 0.05, we adjust ω_A^C as $\omega_A^C/2\pi = 0.7$ GHz, 0.6 GHz, 0.55 GHz, and accordingly, χ_{conf} changes as $\chi_{\mathrm{conf}} = 399$, 248, 139, respectively [61].

significantly confined to the E2LS as $n_{\mathrm{conf}} = 1/[a_{-1/2}(\Gamma^{H\downarrow}_{-1/2}\tau_H + \Gamma^{C\downarrow}_{-1/2}\tau_C)] \simeq [1 + 16(\Omega/\Delta\omega)^2]/(2\varepsilon)$. For our settings, $n_{\mathrm{conf}} \simeq 7.69 \times 10^6$. Second, for $\Delta\eta_{\mathrm{E2LS}} = 0.05$ and $N = 31$, we numerically calculate $\Delta\eta$ and P for $5000(\ll n_{\mathrm{conf}})$ heat engine cycles, and we find that the results deviate from $\Delta\eta_{\mathrm{E2LS}}$ and P_{E2LS} only by a few percent at most, respectively (the detailed settings are given in the caption of Fig. 2). From these results, we conclude that the confinement in the E2LS is sufficiently strong to claim that we approximately have a closed trajectory of the quantum state after each cycle. Finally, we numerically calculate the power output $P(N)$ against N with several values of ω_A^C. As we fix the other parameters, the change in ω_A^C induces the change in $\Delta\eta_{\mathrm{E2LS}}$. We plot the power outputs against the number of qubits, as shown in Fig. 2. Here, we define $P(N)$ as the power output of the first cycle for each N. As $\Delta\eta_{\mathrm{E2LS}}$ decreases, the power P decreases for the fixed N. However, importantly, the behavior $P = \Theta(N^2)$ is observed regardless of the value of $\Delta\eta_{\mathrm{E2LS}}$. Therefore, for a large number of qubits, we can achieve both high power and high efficiency in our engine with entanglement, compared with the conventional engine with separable states.

Conclusion.—We proposed a quantum-enhanced heat engine with a power output that exhibits a quantum scaling with the number of qubits at a finite temperature. Our engine is fueled by an entanglement-enhanced energy absorption process called superabsorption, where the dynamics of an N-qubit system is approximately confined in a subspace spanned by two highly entangled states. We analytically showed that, as long as the confinement is significant, our engine achieves a power of $P = \Theta(N^2)$ with N entangled qubits, whereas a conventional engine with N separable qubits provides a power of $P = \Theta(N)$. Moreover, we numerically observed the same scaling advantage even under the effect of a finite leakage to the other states. We elucidate the mechanism of quantum enhancement of performance, and show that a connectivity of the quantum states between one degenerated subspace and another induced by the system-environment interaction plays an important role in achieving the scaling advantage with the quantum heat engine. Our proposal is also important for realizing next-generation quantum devices such as high-performance refrigerators for quantum systems [83–85].

We thank H. Tajima and K. Funo for their insightful feedback. We also thank an anonymous reviewer for invaluable comments regarding the importance of connectivity. This work was supported by MEXT's Leading Initiative for Excellent Young Researchers, JST COI-NEXT program (JPMJPF2014) and JST PRESTO (Grant No. JPMJPR1919), Japan. Y. T. acknowledges support from JSPS KAKENHI (No. 20H01827) and JST's Moonshot R&D (Grant No. JPMJMS2061).

Note added.—Recently, we became aware of a related study that uses a collective effect for a quantum refrigerator [86].

*s2130043@s.tsukuba.ac.jp
†matsuzaki.yuichiro@aist.go.jp
‡tokura.yasuhiro.ft@u.tsukuba.ac.jp

[1] P. W. Shor, Algorithms for quantum computation: discrete logarithms and factoring, *Proceedings of the 35th Annual Symposium on Foundations of Computer Science* (IEEE, New York, 1994), pp. 124–134, https://ieeexplore.ieee.org/abstract/document/365700.
[2] L. K. Grover, Quantum Mechanics Helps in Searching for a Needle in a Haystack, Phys. Rev. Lett. **79**, 325 (1997).
[3] A. W. Harrow, A. Hassidim, and S. Lloyd, Quantum Algorithm for Linear Systems of Equations, Phys. Rev. Lett. **103**, 150502 (2009).
[4] S. F. Huelga, C. Macchiavello, T. Pellizzari, A. K. Ekert, M. B. Plenio, and J. I. Cirac, Improvement of Frequency Standards with Quantum Entanglement, Phys. Rev. Lett. **79**, 3865 (1997).
[5] V. Giovannetti, S. Lloyd, and L. Maccone, Advances in quantum metrology, Nat. Photonics **5**, 222 (2011).
[6] C. L. Degen, F. Reinhard, and P. Cappellaro, Quantum sensing, Rev. Mod. Phys. **89**, 035002 (2017).
[7] S. Carnot, Réflexions sur la puissance motrice du feu et sur les machines propres à développer cette puissance Front Cover, Ann. Sci. Éc. Norm. Supér. **1**, 393 (1872).
[8] H. B. Callen, *Thermodynamics and an Introduction to Thermostatistics*, 2nd ed. (Wiley, New York, 1985).
[9] U. Seifert, Stochastic thermodynamics, fluctuation theorems and molecular machines, Rep. Prog. Phys. **75**, 126001 (2012).

[10] R. Landauer, Irreversibility and heat generation in the computing process, IBM J. Res. Dev. **5**, 183 (1961).
[11] T. Sagawa and M. Ueda, Second Law of Thermodynamics with Discrete Quantum Feedback Control, Phys. Rev. Lett. **100**, 080403 (2008).
[12] J. M. Parrondo, J. M. Horowitz, and T. Sagawa, Thermodynamics of information, Nat. Phys. **11**, 131 (2015).
[13] C. Jarzynski, Nonequilibrium Equality for Free Energy Differences, Phys. Rev. Lett. **78**, 2690 (1997).
[14] G. E. Crooks, Entropy production fluctuation theorem and the nonequilibrium work relation for free energy differences, Phys. Rev. E **60**, 2721 (1999).
[15] T. Hatano and S.-i. Sasa, Steady-State Thermodynamics of Langevin Systems, Phys. Rev. Lett. **86**, 3463 (2001).
[16] U. Seifert, Entropy Production along a Stochastic Trajectory and an Integral Fluctuation Theorem, Phys. Rev. Lett. **95**, 040602 (2005).
[17] N. Shiraishi, K. Saito, and H. Tasaki, Universal Trade-Off Relation between Power and Efficiency for Heat Engines, Phys. Rev. Lett. **117**, 190601 (2016).
[18] P. Pietzonka and U. Seifert, Universal Trade-Off between Power, Efficiency, and Constancy in Steady-State Heat Engines, Phys. Rev. Lett. **120**, 190602 (2018).
[19] K. Sekimoto, *Stochastic Energetics* (Springer, New York, 2010), Vol. 799, https://link.springer.com/book/10.1007/978-3-642-05411-2.
[20] R. Rao and M. Esposito, Nonequilibrium Thermodynamics of Chemical Reaction Networks: Wisdom from Stochastic Thermodynamics, Phys. Rev. X **6**, 041064 (2016).
[21] C. Jarzynski, The thermodynamics of writing a random polymer, Proc. Natl. Acad. Sci. U.S.A. **105**, 9451 (2008).
[22] D. Andrieux and P. Gaspard, Nonequilibrium generation of information in copolymerization processes, Proc. Natl. Acad. Sci. U.S.A. **105**, 9516 (2008).
[23] S. Vinjanampathy and J. Anders, Quantum thermodynamics, Contemp. Phys. **57**, 545 (2016).
[24] S. Deffner and S. Campbell, *Quantum Thermodynamics: An Introduction to the Thermodynamics of Quantum Information* (Morgan & Claypool Publishers, San Rafael, 2019).
[25] F. Binder, L. A. Correa, C. Gogolin, J. Anders, and G. Adesso, Thermodynamics in the Quantum Regime, Fund. Theor. Phys. **195**, 1 (2018).
[26] R. Alicki, The quantum open system as a model of the heat engine, J. Phys. A **12**, L103 (1979).
[27] H.-T. Quan, Y.-x. Liu, C.-P. Sun, and F. Nori, Quantum thermodynamic cycles and quantum heat engines, Phys. Rev. E **76**, 031105 (2007).
[28] P. Talkner, E. Lutz, and P. Hänggi, Fluctuation theorems: Work is not an observable, Phys. Rev. E **75**, 050102(R) (2007).
[29] C. Bergenfeldt, P. Samuelsson, B. Sothmann, C. Flindt, and M. Büttiker, Hybrid Microwave-Cavity Heat Engine, Phys. Rev. Lett. **112**, 076803 (2014).
[30] K. Zhang, F. Bariani, and P. Meystre, Quantum Optomechanical Heat Engine, Phys. Rev. Lett. **112**, 150602 (2014).
[31] J. P. Pekola, Towards quantum thermodynamics in electronic circuits, Nat. Phys. **11**, 118 (2015).
[32] F. Altintas, A. Ü. C. Hardal, and Ö. E. Müstecaplıoğlu, Rabi model as a quantum coherent heat engine: From quantum biology to superconducting circuits, Phys. Rev. A **91**, 023816 (2015).
[33] J. P. S. Peterson, T. B. Batalhão, M. Herrera, A. M. Souza, R. S. Sarthour, I. S. Oliveira, and R. M. Serra, Experimental Characterization of a Spin Quantum Heat Engine, Phys. Rev. Lett. **123**, 240601 (2019).
[34] K. E. Dorfman, D. V. Voronine, S. Mukamel, and M. O. Scully, Photosynthetic reaction center as a quantum heat engine, Proc. Natl. Acad. Sci. U.S.A. **110**, 2746 (2013).
[35] H. Tajima and K. Funo, Superconducting-like Heat Current: Effective Cancellation of Current-Dissipation Trade-Off by Quantum Coherence, Phys. Rev. Lett. **127**, 190604 (2021).
[36] A. Ü. C. Hardal and Ö. E. Müstecaplıoğlu, Superradiant Quantum Heat Engine, Sci. Rep. **5**, 12953 (2015).
[37] W. Niedenzu and G. Kurizki, Cooperative many-body enhancement of quantum thermal machine power, New J. Phys. **20**, 113038 (2018).
[38] M. Kloc, P. Cejnar, and G. Schaller, Collective performance of a finite-time quantum Otto cycle, Phys. Rev. E **100**, 042126 (2019).
[39] G. Watanabe, B. P. Venkatesh, P. Talkner, M.-J. Hwang, and A. del Campo, Quantum Statistical Enhancement of the Collective Performance of Multiple Bosonic Engines, Phys. Rev. Lett. **124**, 210603 (2020).
[40] K. Higgins, S. Benjamin, T. Stace, G. Milburn, B. W. Lovett, and E. Gauger, Superabsorption of light via quantum engineering, Nat. Commun. **5**, 4705 (2014).
[41] A. Mirzaei, I. V. Shadrivov, A. E. Miroshnichenko, and Y. S. Kivshar, Superabsorption of light by multilayer nanowires, Nanoscale **7**, 17658 (2015).
[42] W. M. Brown and E. M. Gauger, Light harvesting with guide-slide superabsorbing condensed-matter nanostructures, J. Phys. Chem. Lett. **10**, 4323 (2019).
[43] D. Yang, S.-h. Oh, J. Han, G. Son, J. Kim, J. Kim, M. Lee, and K. An, Realization of superabsorption by time reversal of superradiance, Nat. Photonics **15**, 272 (2021).
[44] N. Shiraishi and K. Saito, Fundamental relation between entropy production and heat current, J. Stat. Phys. **174**, 433 (2019).
[45] R. H. Dicke, Coherence in spontaneous radiation processes, Phys. Rev. **93**, 99 (1954).
[46] N. E. Rehler and J. H. Eberly, Superradiance, Phys. Rev. A **3**, 1735 (1971).
[47] M. Gross and S. Haroche, Superradiance: An essay on the theory of collective spontaneous emission, Phys. Rep. **93**, 301 (1982).
[48] T. Brandes, Coherent and collective quantum optical effects in mesoscopic systems, Phys. Rep. **408**, 315 (2005).
[49] U. Fano, Effects of configuration interaction on intensities and phase shifts, Phys. Rev. **124**, 1866 (1961).
[50] K. Koshino and A. Shimizu, Quantum Zeno effect by general measurements, Phys. Rep. **412**, 191 (2005).
[51] E. Purcell, Resonance absorption by nuclear magnetic moments in a solid, Phys. Rev. **69** (1946).
[52] A. Bienfait, J. Pla, Y. Kubo, X. Zhou, M. Stern, C. Lo, C. Weis, T. Schenkel, D. Vion, D. Esteve *et al.*, Controlling spin relaxation with a cavity, Nature (London) **531**, 74 (2016).

[53] S. Campbell, M. Tame, and M. Paternostro, Characterizing multipartite symmetric Dicke states under the effects of noise, New J. Phys. **11**, 073039 (2009).
[54] P. Hyllus, O. Gühne, and A. Smerzi, Not all pure entangled states are useful for sub-shot-noise interferometry, Phys. Rev. A **82**, 012337 (2010).
[55] G. Tóth, Multipartite entanglement and high-precision metrology, Phys. Rev. A **85**, 022322 (2012).
[56] C. Wu, C. Guo, Y. Wang, G. Wang, X.-L. Feng, and J.-L. Chen, Generation of Dicke states in the ultrastrong-coupling regime of circuit QED systems, Phys. Rev. A **95**, 013845 (2017).
[57] S. Kasture, Scalable approach to generation of large symmetric Dicke states, Phys. Rev. A **97**, 043862 (2018).
[58] H. Hakoshima and Y. Matsuzaki, Efficient detection of inhomogeneous magnetic fields from a single spin with Dicke states, Phys. Rev. A **102**, 042610 (2020).
[59] H. Kasai, Y. Takeuchi, H. Hakoshima, Y. Matsuzaki, and Y. Tokura, Anonymous quantum sensing, arXiv:2105.05585.
[60] P. Goy, J. M. Raimond, M. Gross, and S. Haroche, Observation of Cavity-Enhanced Single-Atom Spontaneous Emission, Phys. Rev. Lett. **50**, 1903 (1983).
[61] See Supplemental Material at http://link.aps.org/supplemental/10.1103/PhysRevLett.128.180602 for some details, which includes Refs. [62–82].
[62] A. Streltsov, G. Adesso, and M. B. Plenio, Colloquium: Quantum coherence as a resource, Rev. Mod. Phys. **89**, 041003 (2017).
[63] J. Clarke and F. K. Wilhelm, Superconducting quantum bits, Nature (London) **453**, 1031 (2008).
[64] F. G. Paauw, A. Fedorov, C. J. P. M Harmans, and J. E. Mooij, Tuning the Gap of a Superconducting Flux Qubit, Phys. Rev. Lett. **102**, 090501 (2009).
[65] X. Zhu, A. Kemp, S. Saito, and K. Semba, Coherent operation of a gap-tunable flux qubit, Appl. Phys. Lett. **97**, 102503 (2010).
[66] R. Harris, M. W. Johnson, T. Lanting, A. J. Berkley, J. Johansson, P. Bunyk, E. Tolkacheva, E. Ladizinsky, N. Ladizinsky, T. Oh *et al.*, Experimental investigation of an eight-qubit unit cell in a superconducting optimization processor, Phys. Rev. B **82**, 024511 (2010).
[67] R. Harris, J. Johansson, A. J. Berkley, M. W. Johnson, T. Lanting, S. Han, P. Bunyk, E. Ladizinsky, T. Oh, I. Perminov *et al.*, Experimental demonstration of a robust and scalable flux qubit, Phys. Rev. B **81**, 134510 (2010).
[68] A. A. Abdumalikov Jr, O. Astafiev, Y. Nakamura, Y. A. Pashkin, and J. S. Tsai, Vacuum Rabi splitting due to strong coupling of a flux qubit and a coplanar-waveguide resonator, Phys. Rev. B **78**, 180502(R) (2008).
[69] T. Yamamoto, K. Inomata, K. Koshino, P. Billangeon, Y. Nakamura, and J. Tsai, Superconducting flux qubit capacitively coupled to an LC resonator, New J. Phys. **16**, 015017 (2014).
[70] T. Lindström, C. Webster, J. Healey, M. Colclough, C. Muirhead, and A. Y. Tzalenchuk, Circuit QED with a flux qubit strongly coupled to a coplanar transmission line resonator, Supercond. Sci. Technol. **20**, 814 (2007).
[71] J. Johansson, S. Saito, T. Meno, H. Nakano, M. Ueda, K. Semba, and H. Takayanagi, Vacuum Rabi Oscillations in a Macroscopic Superconducting Qubit *LC* Oscillator System, Phys. Rev. Lett. **96**, 127006 (2006).
[72] I. Chiorescu, P. Bertet, K. Semba, Y. Nakamura, C. Harmans, and J. Mooij, Coherent dynamics of a flux qubit coupled to a harmonic oscillator, Nature (London) **431**, 159 (2004).
[73] P. Macha, G. Oelsner, J.-M. Reiner, M. Marthaler, S. André, G. Schön, U. Hübner, H.-G. Meyer, E. Ilichev, and A. V. Ustinov, Implementation of a quantum metamaterial using superconducting qubits, Nat. Commun. **5**, 5146 (2014).
[74] K. Kakuyanagi, Y. Matsuzaki, C. Déprez, H. Toida, K. Semba, H. Yamaguchi, W. J. Munro, and S. Saito, Observation of Collective Coupling between an Engineered Ensemble of Macroscopic Artificial Atoms and a Superconducting Resonator, Phys. Rev. Lett. **117**, 210503 (2016).
[75] F. Yan, S. Gustavsson, A. Kamal, J. Birenbaum, A. P. Sears, D. Hover, T. J. Gudmundsen, D. Rosenberg, G. Samach, S. Weber *et al.*, The flux qubit revisited to enhance coherence and reproducibility, Nat. Commun. **7**, 1 (2016).
[76] J. Bylander, S. Gustavsson, F. Yan, F. Yoshihara, K. Harrabi, G. Fitch, D. G. Cory, Y. Nakamura, J.-S. Tsai, and W. D. Oliver, Noise spectroscopy through dynamical decoupling with a superconducting flux qubit, Nat. Phys. **7**, 565 (2011).
[77] L. V. Abdurakhimov, I. Mahboob, H. Toida, K. Kakuyanagi, and S. Saito, A long-lived capacitively shunted flux qubit embedded in a 3D cavity, Appl. Phys. Lett. **115**, 262601 (2019).
[78] H. Mukai, K. Sakata, S. J. Devitt, R. Wang, Y. Zhou, Y. Nakajima, and J.-S. Tsai, Pseudo-2D superconducting quantum computing circuit for the surface code: proposal and preliminary tests, New J. Phys. **22**, 043013 (2020).
[79] M. Reagor, W. Pfaff, C. Axline, R. W. Heeres, N. Ofek, K. Sliwa, E. Holland, C. Wang, J. Blumoff, K. Chou *et al.*, Quantum memory with millisecond coherence in circuit QED, Phys. Rev. B **94**, 014506 (2016).
[80] V. Sevriuk, K. Y. Tan, E. Hyyppä, M. Silveri, M. Partanen, M. Jenei, S. Masuda, J. Goetz, V. Vesterinen, L. Grönberg, and M. Möttönen, Fast control of dissipation in a superconducting resonator, Appl. Phys. Lett. **115**, 082601 (2019).
[81] F. Yoshihara, T. Fuse, S. Ashhab, K. Kakuyanagi, S. Saito, and K. Semba, Superconducting qubit–cillator circuit beyond the ultrastrong-coupling regime, Nat. Phys. **13**, 44 (2017).
[82] A. Blais, R.-S. Huang, A. Wallraff, S. M. Girvin, and R. J. Schoelkopf, Cavity quantum electrodynamics for superconducting electrical circuits: An architecture for quantum computation, Phys. Rev. A **69**, 062320 (2004).
[83] R. Kosloff and A. Levy, Quantum heat engines and refrigerators: continuous devices, Annu. Rev. Phys. Chem. **65**, 365 (2014).
[84] N. Brunner, M. Huber, N. Linden, S. Popescu, R. Silva, and P. Skrzypczyk, Entanglement enhances cooling in microscopic quantum refrigerators, Phys. Rev. E **89**, 032115 (2014).
[85] K. Y. Tan, M. Partanen, R. E. Lake, J. Govenius, S. Masuda, and M. Möttönen, In situ click chemistry generation of cyclooxygenase-2 inhibitors, Nat. Commun. **8**, 1 (2017).
[86] M. Kloc, K. Meier, K. Hadjikyriakos, and G. Schaller, Superradiant Many-Qubit Absorption Refrigerator, Phys. Rev. Applied **16**, 044061 (2021).